

## Electronic structure of the [001] InAs-GaSb superlattice

J. Ihm, Pui K. Lam, and Marvin L. Cohen\*

*Department of Physics, University of California, Berkeley, California 94720*

*and Materials and Molecular Research Division, Lawrence Berkeley Laboratory, Berkeley, California 94720*

(Received 11 June 1979)

The self-consistent pseudopotential method has been applied to describe the electronic structure of the abrupt [001] InAs-GaSb superlattice. According to the electron affinity rule, the bottom of the conduction band of InAs lies below the top of the valence band of GaSb. Consequently, physically interesting phenomena have been expected for this system. Since the possible charge redistribution at the junction determines the dipole potential and the relative lineup of the band edges, self-consistency in charge distribution is required of a quantitative theory of a superlattice. The calculated band-edge lineup, band dispersions, and the electronic configuration at the junction are presented and discussed.

### I. INTRODUCTION

A series of recent experiments on the [001] InAs-GaSb superlattice<sup>1-5</sup> has revealed many interesting properties of this system, e.g., the quasi-two-dimensional subbands, charge-confinement effects, and the semiconductor-semimetal transition. Most notably, Sakaki *et al.*<sup>1</sup> claimed that they observed the transition from rectifying to ohmic behavior of the  $\text{InGa}_x\text{As}_{1-x}\text{-GaAs}_y\text{Sb}_{1-y}$  superlattice, with varying  $x$  and  $y$ , prepared by the molecular-beam-epitaxy technique. On the theoretical side, after the Kronig-Penney model potential had been considered,<sup>6</sup> a one-dimensional tight-binding calculation was done by Sai-Halasz *et al.*<sup>7</sup> These authors were mainly interested in investigating the possible semiconductor-semimetal transition as a function of the unit-supercell size. A more realistic three-dimensional tight-binding calculation has been done by Madhukar *et al.*,<sup>8</sup> focusing on a study of the two-dimensional effects and effective masses.

The aim of the present self-consistent pseudopotential calculation is to derive the band structure and the microscopic electronic structure of the superlattice in a more fundamental way, i.e., without fitting to the known band structure of each bulk material. The only input data of our calculation are the ionic pseudopotentials of In, As, Ga, and Sb derived from the respective all-electron atomic calculations. These ionic pseudopotentials for isolated atoms, when screened self-consistently, reproduce the atomic-term values and the shape of the atomic wave functions outside the core region for In, As, Ga, and Sb. These pseudopotentials are then used to determine the self-consistent electronic structure in the superlattice geometry. Because the large unit-supercell size requires considerable computing time, we have not considered the effects of the spin-orbit inter-

action in the calculation itself. The projected band structure of the system, the band-edge lineup, and the microscopic charge distribution for each eigenstate are obtained. The dispersion of bands along the direction perpendicular to the interface (IF) plane enables us to evaluate the effective masses, thereby deducing transport properties of the superlattice. Moreover, properties of the superlattice of varying unit-cell thickness (4, 12, and 24 layers) have been studied to extract gross trends of these properties as a function of thickness.

The calculational procedure will be briefly described in the next section, and the last two sections will be devoted to the presentation of the results and discussions.

### II. CALCULATIONS

The self-consistent pseudopotential method with superlattice geometry has been discussed extensively elsewhere.<sup>9</sup> The ionic pseudopotential representing the *effective* core-valence interaction is derived by fitting to the all-electron atomic term values and atomic valence wave functions. We do not assume any parametrized form for the pseudopotential; rather, we use a "first-principle-like pseudopotential"<sup>10</sup> with the restriction that it vanish in momentum ( $q$ ) space if  $q$  is larger than 3 (in atomic units). This restriction enables us to maintain a manageable matrix size in solving the Schrödinger equation for a large superlattice. Figure 1 shows the ionic pseudopotentials of the atoms in real space. Although nonlocal pseudopotentials have been obtained for the elements used here, we have used averaged local potentials to simplify the computation. These potentials are smooth near the origin and approach  $-2Z_v/r$  (in Rydberg atomic units) for large  $r$ , where  $Z_v$  is the valence of each species. The calculated pseudo wave functions and eigenvalues of the atoms are compared with the corresponding all-electron

TABLE I. Peaks and eigenvalues of the pseudovalence wave functions calculated from the pseudopotentials in Fig. 1 compared with corresponding all-electron (a.e.) local-density-functional calculations ( $\alpha = \frac{2}{3}$ ). The position of the maximum of the  $r\psi(r)$  from the origin agrees to within 10%, and the normalized value of  $r\psi(r)$  at the maximum agrees to within a few percent. The tabulated peak position of each a.e. calculation refers to the outermost peak. The pseudo wave function has only one peak. The last two columns contain a comparison of term values.

		Peak position ( $a_B$ )		Peak value (normalized)		Term value (Ry)	
		a.e.	pseudo	a.e.	pseudo	a.e.	pseudo
In	5s	2.216	2.216	0.6774	0.6902	-0.5078	-0.5062
	5p	2.845	2.511	0.5387	0.5488	-0.1423	-0.1486
As	4s	1.654	1.761	0.7924	0.7686	-0.9627	-0.9774
	4p	2.000	2.124	0.6597	0.6821	-0.3178	-0.3223
Ga	4s	1.996	1.996	0.7035	0.7116	-0.5819	-0.5914
	4p	2.563	2.407	0.5455	0.5571	-0.1413	-0.1409
Sb	5s	2.000	2.000	0.7512	0.7656	-0.8094	-0.7840
	5p	2.413	2.266	0.6358	0.6797	-0.2968	-0.3190

results in Table I. The peak of the valence wave function occurs in the correct region of space for each case, and the term values for valence s and p states are within 0.3 eV of the all-electron value. Because we are using a local pseudopotential with a small range in momentum space, the Sb atomic term values were difficult to bring into good agreement with the all-electron calculation. Despite this problem, the results for the self-consistently calculated band gap of GaSb at  $\Gamma$  is acceptable (0.99 eV compared with the experimental value of 0.78 eV at 0°K).<sup>11</sup> The calculated band gap for InAs at  $\Gamma$  is 0.51 eV compared with the experimental value of 0.43 eV (0°K).<sup>11</sup> The agreement would be improved considerably if spin-orbit splitting<sup>11,12</sup> were incorporated in our calculation.

The structure of the superlattice in the IF re-

gion is shown schematically in Fig. 2. Here, the IF between the As plane and the Ga plane is shown. It is also possible to form an IF between In and Sb. Three separate calculations are done: (2-2) layers (namely, the InAsGaSb quaternary compound), (6-6) layers, and (12-12) layers. The wave functions are expanded in terms of plane waves with kinetic energies up to 2.8 Ry. This value corresponds to 120, 350, and 700 plane waves for the (2-2), (6-6), and (12-12) layers, respectively. Another set of plane waves up to 5.5 Ry in kinetic energy, corresponding to 180, 550, and 1100 plane waves, is included through second-order perturbation. The statistical exchange potential with  $\alpha = \frac{2}{3}$  is used, and self-consistency is achieved to within 0.01 eV for both the eigenvalues and the components of the screening potential.

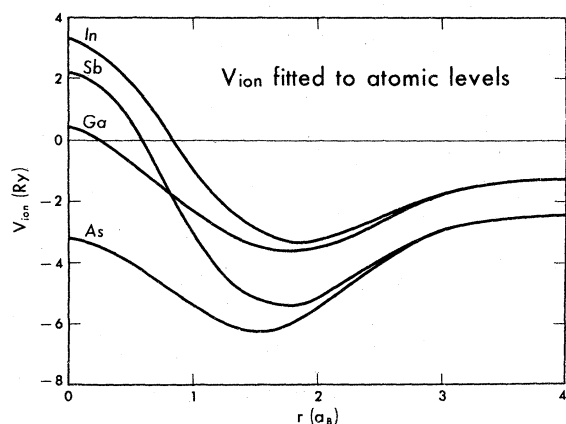


FIG. 1. Ionic pseudopotentials of the In, As, Ga, and Sb atom near the core region. These potentials vary as  $-2Z_v/r$  (in Rydberg atomic units) for large  $r$ , where  $Z_v$  is the valence of each species.

Structure of InAs-GaSb superlattice

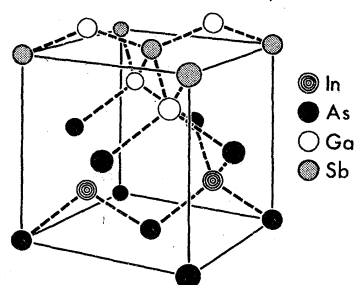


FIG. 2. Atomic positions near the [001] InAs-GaSb IF. Hypothetical bonds are drawn as dashed lines. This figure represents the IF between As and Ga, which is one of the two possible IF's in the [001] InAs-GaSb superlattice.

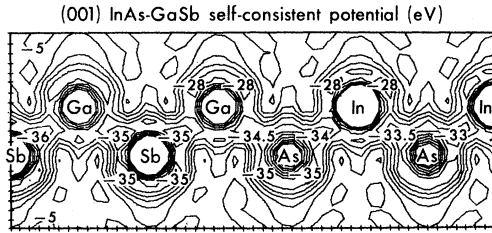


FIG. 3. Total self-consistent potential of the [001] InAs-GaSb superlattice (with a 24-layer unit cell) is shown in the IF region. Energies are in eV. The potential contours inside the core (which are not accurately given in the pseudopotential formalism) are left out for clarity.

### III. RESULTS

The basic results of the present calculation can be summarized in terms of Figs. 3-9. The results presented here are mostly for the (12-12) geometry. Some discussion will be given on the comparison with smaller superlattices [(2-2) and (6-6) layers] whenever the comparison is relevant. Figure 3 shows the total self-consistent potential (including the screening potential) of the (12-12) geometry near the IF region. The bulk periodicity of the potential on each side is restored within two layers of atoms away from the IF; the perturbation due to the IF is rapidly reduced by electron screening. The total (pseudo) valence charge density of the superlattice is shown in Fig. 4. Two layers away from the IF the charge density of the (12-12) superlattice is similar to bulk InAs or bulk GaSb, respectively. To illustrate how effectively the electronic redistribution screens the perturbation at the IF, the total potential averaged parallel to the IF is shown in Fig. 5(a) (plotted perpendicular to the IF). The average potential with (12-12) layers is superim-

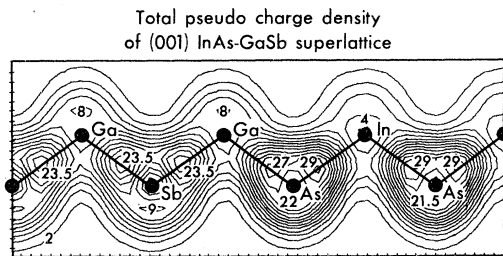


FIG. 4. Total (pseudo) valence charge density of the [001] InAs-GaSb superlattice. Atomic positions are denoted by solid circles and the hypothetical covalent bonds are represented as solid lines. Normalization is fixed by the number of electrons per bulk unit cell (378.434 a.u.).

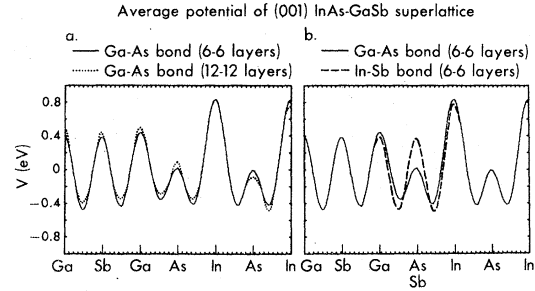


FIG. 5. Total self-consistent potentials  $V(z)$  averaged parallel to the IF plane and plotted perpendicular to it: (a) comparison between the 12-layer unit cell and the 24-layer unit cell. Maximum difference in the two curves is  $<0.05$  eV. (b) Comparison between the Ga-As bond and the In-Sb bond. The two curves are within 0.03 eV of each other at a distance of more than one layer away from the IF. Dashed curves are left out wherever two curves are separated by less than 0.02 eV.

posed on the (6-6) layers' result. Nonperiodicity of the potential is limited to a narrow region at the IF. More importantly, the overall agreement between the two cases is within 0.05 eV. Agreement is even better (0.02 eV) in the bulk region (away from the IF). This means that (6-6) layers reproduce the same screening as thicker (12-12)

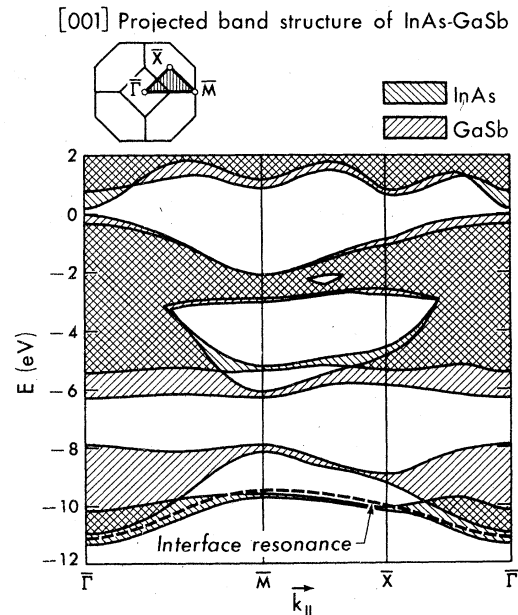


FIG. 6. Band structures of InAs and GaSb projected along the [001] direction based on the present self-consistent calculation. The dispersion of the IF resonance is represented by a dashed line. Weak IF resonances confined to symmetry points ( $M$  and  $X$ ) are not presented in the figure. The two-dimensional Brillouin zone is also shown.

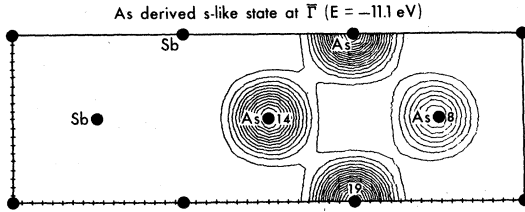


FIG. 7. Contour plot, perpendicular to the IF, of the charge density of the IF resonance at  $\bar{\Gamma}$ . This is an As-derived s-like state localized within two As layers of the IF. Atomic positions are indicated by solid circles. Normalization is fixed by the number of electrons per unit superlattice.

layers do, which in turn indicates that the screening is convergent up to 0.02 eV at least within three layers (three rather than six because one material experiences perturbation from contact with the other material on both sides).

Since the [001] surface is a polar face of the crystal, there are two possible IF's between InAs and GaSb: the Ga-As and the In-Sb IF. Experiments show that the Ga-As IF is the one usually found. This observation will be discussed in the last section in connection with relaxation effects. In fact, two separate self-consistent calculations were done—one with Ga-As bonds only (four As and two Sb layers in the case of 6-6 layers) and the other with In-Sb bonds only (four Sb and two As layers). Since there are different atoms at the IF for the two cases, differences in the charge

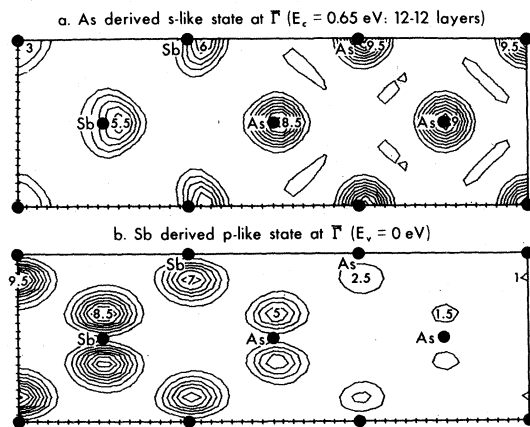


FIG. 8. Contour plots, perpendicular to the IF, of the charge densities of the 24-layer superlattice states near the gap: (a) state at the bottom of the conduction band (at  $\bar{\Gamma}$ ) and (b) state at the top of the valence band (at  $\bar{\Gamma}$ ). The charge confinement to one side and the exponential decay of the charge to the other side are well illustrated in the figure. Normalization is the same as in Fig. 7.

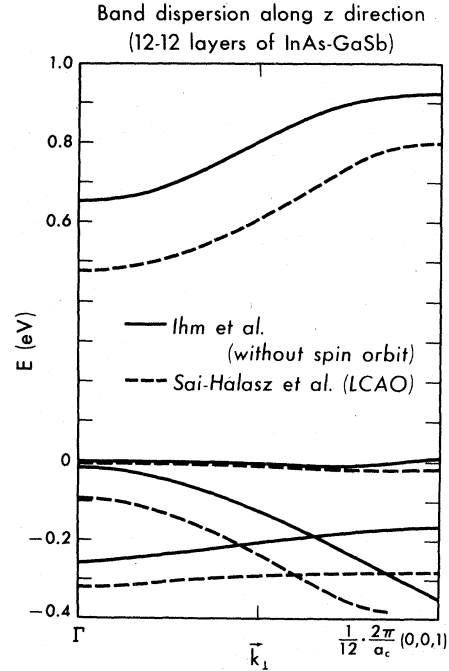


FIG. 9. Dispersion of the 24-layer superlattice sub-bands along the perpendicular direction to the IF. Bands are shown near the gap region and compared with the tight-binding calculation in Ref. 7.

distribution at the IF between the two cases are quite noticeable. In Fig. 5(b) the average potentials in the IF region with Ga-As bonds and In-Sb bonds are compared. The relative lineup of the two bulk potentials across the IF (InAs is  $\sim 0.3$  eV higher than GaSb; this is a measure of the IF dipole potential.) is shown to be the same up to 0.02 eV whether we have Ga-As bonds or In-Sb bonds at the IF. This indicates that, although the charge redistribution occurs within a very narrow region of the IF, the change in the average potential arising from the electronic redistribution (namely, the formation of the potential barrier across the IF) is determined essentially by the bulk properties of the constituent materials rather than by the detailed configuration of the IF. Of course, this observation depends in part on the similarity of GaAs and InSb.

The bulk band structures of InAs and GaSb projected along the [001] direction are plotted in Fig. 6. The relative lineup between the InAs and the GaSb band has been determined from the self-consistent potential of the superlattice. The projected band structure shows that the conduction-band minimum of InAs is 0.21 eV above the valence-band maximum of GaSb in the thick-layers limit. However, we have not included spin-orbit interac-

tions as yet. The spin-orbit splitting at the valence-band maximum of GaSb is  $\sim 0.8$  eV,<sup>12</sup> and hence the spin-orbit interaction can change our results. If it were not for interactions with the conduction band of InAs, the sixfold degenerate states (including spin degeneracy) of GaSb at the valence-band maximum would be split off by the spin-orbit interactions into spin- $\frac{3}{2}$  states 0.27 eV above and spin- $\frac{1}{2}$  states 0.53 eV below the original energy level. However, the conduction band of InAs is very close to the valence band of GaSb in energy and interaction between them can modify the energy levels significantly.

In Fig. 6 the IF resonance band is represented by a dashed line. The contour plot of the charge density corresponding to the IF resonance at  $\bar{\Gamma}$  is shown in Fig. 7. The state is As-derived s-like and it is well localized at the IF. This figure illustrates the region near the Ga-As bond. We have also found resonant states of the same character (As derived) and of the same degree of charge localization for the IF with the In-Sb bond. Electrons here are localized one layer below the IF on the InAs side since it is As derived. In Fig. 6 the IF resonances split off from the bulk bands and become weak IF states in some region of the Brillouin zone. However, the energy level of this band is sensitive to the self-consistent potential, and it is hard to determine its character unambiguously (between IF resonances and IF states). While the resonances exist near the lower valence band, no IF states or resonances are found in the fundamental gap region. This result is consistent with the tight-binding calculations by Dandekar *et al.*<sup>13</sup> for the [110] InAs-GaSb IF. Since the ionicity change in going from GaSb to InAs is small (0.10 on the Phillips scale<sup>14</sup>), the perturbation at the IF is not strong enough to split off localized states at the IF from the bulk bands. We have found some weakly localized states at band edges of high symmetry points ( $M$  and  $X$ ). Their existence and energy levels depend critically on the self-consistency of the potential, but their contribution to the density of states would be small or perhaps negligible.

In Fig. 8 the (12-12) layers superlattice states at the top of the valence band and at the bottom of the conduction band are illustrated. The charge density contour plot is given in a [100] plane perpendicular to the IF plane. Because the unit superlattice is of finite thickness (24 layers), the gap at  $\bar{\Gamma}$  is larger (0.65 eV) than the thick-layer-limit value (0.21 eV) in the previous figure. This value is the average of the results from the Ga-As IF and the In-Sb IF. States at the top of the valence band are derived mainly from GaSb since the energy level lies within the GaSb bulk band but

above the InAs band. These states are identified with the Sb-derived  $p$ -like states. The charge confinement to the GaSb side is remarkable; this results in a very low tunneling probability and a large effective mass of the hole. The effective masses will be discussed later.

States in the conduction band are derived primarily from InAs because the energy level lies within the InAs bulk band but below the GaSb band. These states may be termed as the As-derived s-like states as shown in the figure. However, the charge confinement to the InAs side is much weaker in this case. There is a significant amount of charge leakage to the GaSb side and a fairly sizable dispersion of the band (i.e., a relatively small electron effective mass) is expected. This is clearly illustrated in Fig. 9, where the dispersion of the (12-12) superlattice bands near the gap region is shown along the direction perpendicular to the IF. As noted above, the top valence band is very flat while the bottom conduction band is quite dispersive. For the (12-12) layers superlattice the electron effective mass in the perpendicular direction ( $m_{xx}$ ) near  $\bar{\Gamma}$  is estimated to be approximately  $0.04 m_e$ . This value is larger than the InAs electron effective mass of  $\sim 0.024 m_e$ , but it is still smaller than the GaSb electron mass of  $\sim 0.048 m_e$ .<sup>6</sup> The top valence band is so flat that it is hard to estimate the hole mass from our calculation. It should be of the order of  $m_e$ . Results from the tight-binding calculation in Ref. 7 are superimposed on the figure. The agreement is good in general. The gap size differs simply because the spin-orbit interaction is not included in the pseudopotential calculation, whereas the tight-binding calculation is fitted to the experimental gap which includes spin-orbit effects. (Madhukar *et al.*<sup>8</sup> have obtained similar results.)

It is expected that the effective mass will increase with an increase in the unit supercell size since a longer unit cell means a smaller overlap. Comparing our (2-2), (6-6), and (12-12) superlattice calculations, no recognizable increase is noted in the electron effective mass at  $\bar{\Gamma}$ , whereas an appreciable increase in the hole effective mass is observed. It is to be noted that the gap size at  $\bar{\Gamma}$  does not change appreciably when the unit cell size increases from 4 to 24 layers. Because we remain in a small unit cell limit even with the 24 layers, it is not possible to derive the behavior of the gap size as a function of the unit cell size. Typical experiments are done with hundreds or thousands of layers.

#### IV. DISCUSSION

Earlier we discussed the importance of the band-edge lineup of the system where the electron

affinity rule predicts an overlap of the conduction band of one material with the valence band of the other by 0.14 eV. This behavior, which is sometimes called a type-II superlattice to be distinguished from a more conventional superlattice like AlAs-GaAs, has been an important stimulus to both experimental and theoretical studies. There has been only one experiment<sup>1</sup> showing direct evidence of the metallic behavior (more precisely, ohmic behavior in the  $I$ - $V$  characteristic). Although tight-binding calculations<sup>7,8</sup> have provided valuable information on many important properties of the superlattice, rigorous theoretical justifications for their approximations (e.g., fixed parameters fitted to individual *bulk* materials) are lacking when the band crossing is about to occur and the self-consistency of the whole electronic structure becomes increasingly important. Therefore, quantitative predictions on the semiconductor-semimetal transition may not be accurate with these methods. The present self-consistent calculations without spin-orbit coupling give a semiconducting superlattice (with a gap size  $\sim 0.21$  eV), and unfortunately, theoretical predictions with spin-orbit coupling are difficult to make at present.

Finally, we consider a possible relaxation or a

reconstruction of the IF. As mentioned earlier, Ga-As bonds are formed predominantly over the In-Sb bonds during experimental preparation. Since a Ga-As bond is  $\sim 7\%$  shorter than an In-As or a Ga-Sb bond, the first-order effect would be the shrinking of the distance between the Ga and As layers by  $\sim 0.34$  Å from the ideal bulk layer separation ( $\sim 1.52$  Å) of InAs or GaSb to assure a bulk GaAs bond length. We may regard such a relaxed geometry as ideal. No significant changes in our results are expected from a relaxation of this amount.<sup>15</sup> The In-Sb bond, being  $\sim 14\%$  longer than the Ga-As bond, would probably be less stable. Saris *et al.*<sup>5</sup> have proposed simultaneous rotation and relaxation of the IF layers to explain Rutherford backscattering and channeling experiments. Little experimental data are yet available regarding the relaxation and the reconstruction of the system.

#### ACKNOWLEDGMENTS

This work was supported by the National Science Foundation (Grant No. DMR7822465) and by the Division of Materials Sciences, Office of Basic Energy Sciences, U.S. Department of Energy (Grant No. W-7405-ENG-48).

\*Guggenheim Fellow 1978-79.

<sup>1</sup>H. Sakaki, L. L. Chang, R. Ludeke, C. A. Chang, G. A. Sai-Halasz, and L. Esaki, *Appl. Phys. Lett.* **31**, 211 (1977).

<sup>2</sup>C. A. Chang, R. Ludeke, L. L. Chang, and L. Esaki, *Appl. Phys. Lett.* **31**, 759 (1977).

<sup>3</sup>H. Sakaki, L. L. Chang, G. A. Sai-Halasz, C. A. Chang, and L. Esaki, *Solid State Commun.* **26**, 589 (1978).

<sup>4</sup>G. A. Sai-Halasz, L. L. Chang, J. M. Welter, C. A. Chang, and L. Esaki (unpublished).

<sup>5</sup>F. W. Saris, C. A. Chang, W. K. Chu, and L. Esaki, in *Proceedings of the Sixth Annual Conference on the Physics of Compound Semiconductor Interfaces*, 1979 (unpublished).

<sup>6</sup>G. A. Sai-Halasz, R. Tsu, and L. Esaki, *Appl. Phys. Lett.* **30**, 651 (1977).

<sup>7</sup>G. A. Sai-Halasz, L. Esaki, and W. A. Harrison, *Phys. Rev. B* **18**, 2812 (1978).

<sup>8</sup>A. Madhukar, N. V. Dandekar, and R. N. Nucho, in *Proceedings of the Sixth Annual Conference on the Physics of Compound Semiconductor Interfaces*, 1979 (unpublished).

<sup>9</sup>M. Schlüter, J. R. Chelikowsky, S. G. Louie, and M. L. Cohen, *Phys. Rev. B* **12**, 4200 (1975); **B** **12**, 5575 (1975); S. G. Louie and M. L. Cohen, *ibid.* **13**, 2461 (1976).

<sup>10</sup>A. Zunger and M. L. Cohen, *Phys. Rev. B* **18**, 5449 (1978).

<sup>11</sup>*Handbook of Chemistry and Physics*, 59th ed., edited by R. C. Weast (Chemical Rubber, Cleveland, 1978), p. E104-5.

<sup>12</sup>See R. N. Cahn and M. L. Cohen, *Phys. Rev. B* **6**, 2569 (1970), and references therein. The experimental spin-orbit splittings for GaSb and InAs at  $\Gamma$  are 0.7-0.8 and 0.43 eV, respectively.

<sup>13</sup>N. V. Dandekar and A. Madhukar, in *Proceedings of the Sixth Annual Conference on the Physics of the Compound Semiconductors*, 1979 (unpublished).

<sup>14</sup>For the table of ionicity values see J. A. van Vechten, *Phys. Rev.* **187**, 1007 (1969).

<sup>15</sup>W. E. Pickett and M. L. Cohen, *Solid State Commun.* **25**, 225 (1978). A relaxation of 20% of the Ge-GaAs IF has been found to result in minor changes in the IF properties.